Electronic Supplementary Information:

A Facile Method to Functionalize Gold Nano-tripods with High Suspension Stability in Aqueous Environment

T.-Y. Tang,‡ H.-L. Wang,‡ C.-T. Yao, K.-C. Yang, R.-M. Ho,† D.-H. Tsai†

Department of Chemical Engineering, National Tsing Hua University, Hsinchu, Taiwan, Republic of China.

† Corresponding Authors. E-mail: dhtsai@mx.nthu.edu.tw; rmho@mx.nthu.edu.tw
‡ Equal contribution

1. Templated synthesis of Au nano-tripods

The PS-templated synthesis of Au nano-tripods followed the procedure described in the previous publications.[1,2] Briefly, the gyroid-structured polymer template from the hydrolysis of a degradable block copolymer thin film, polystyrene (PS)-*b*-poly(L-lactide) (PLLA), was prepared by a double-headed polymerization sequence and the subsequent quenching from microphase-separated ordered melt. After removing the blocks of PLLA by hydrolysis, the BCP thin film became a nanoporous PS template.[2,3] The nanoporous PS template was soaked in a seeding solution composed of hydrogen tetrachloroaurate (III) trihydrate (50 mg) and 20 mL of methanol and stirred for several hours at room temperature. Then 1 mL of hydrazine monohydrate was added into the solution for the nucleation of Au. Subsequently, the PS template of the PS/Au was soaked in a solution mixed with 50 mg of hydrogen tetrachloroaurate(III) trihydrate and 1 ml of diethanolamine and 20 ml of methanol and stirred at room temperature. In this study, the growth time for the fabrication of tripod Au colloid was 7 h. Finally, the redundant Au ions covering on the surface of templates were removed by methanol and DI water.

2. **Additional SEM images**

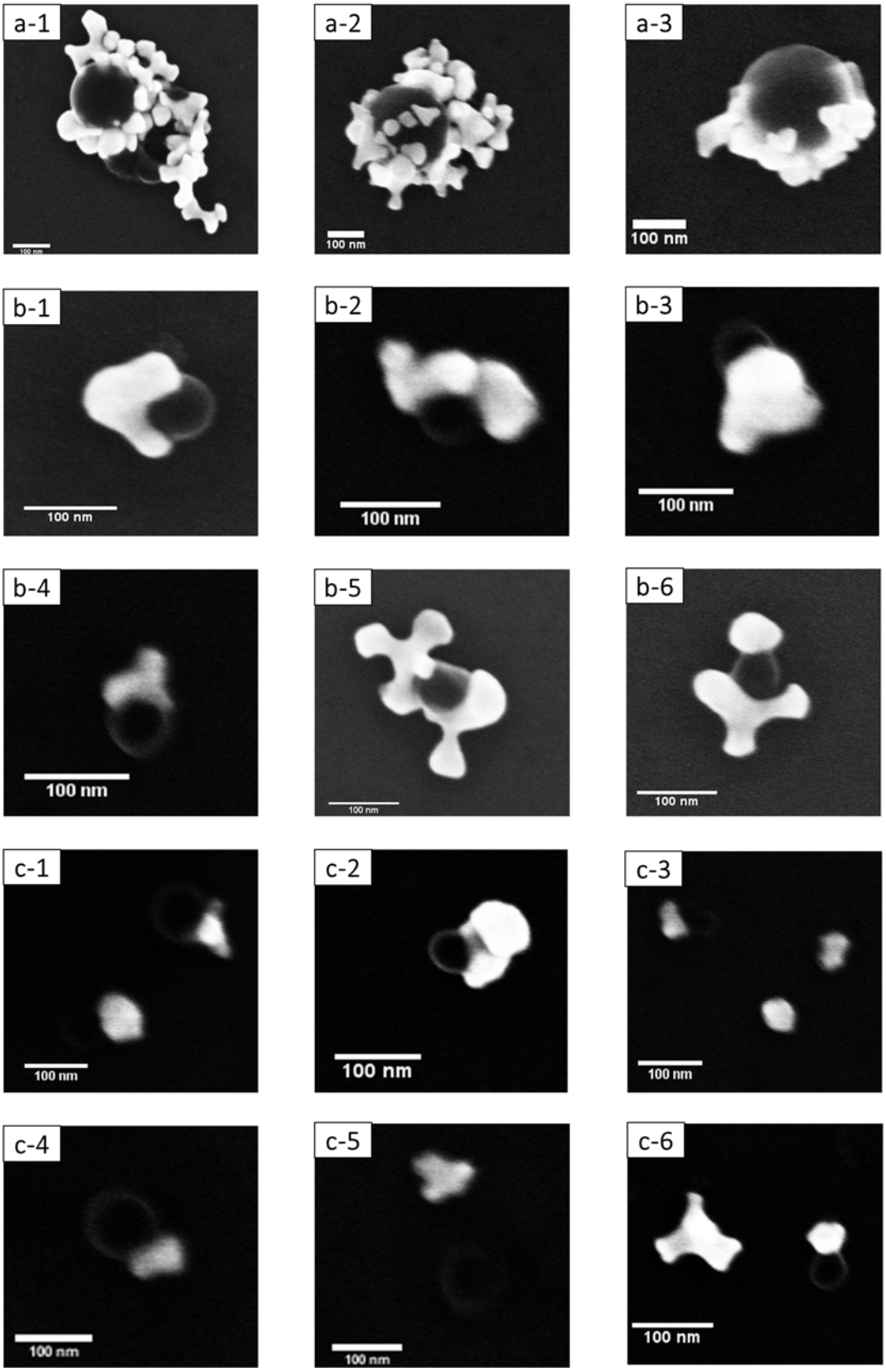

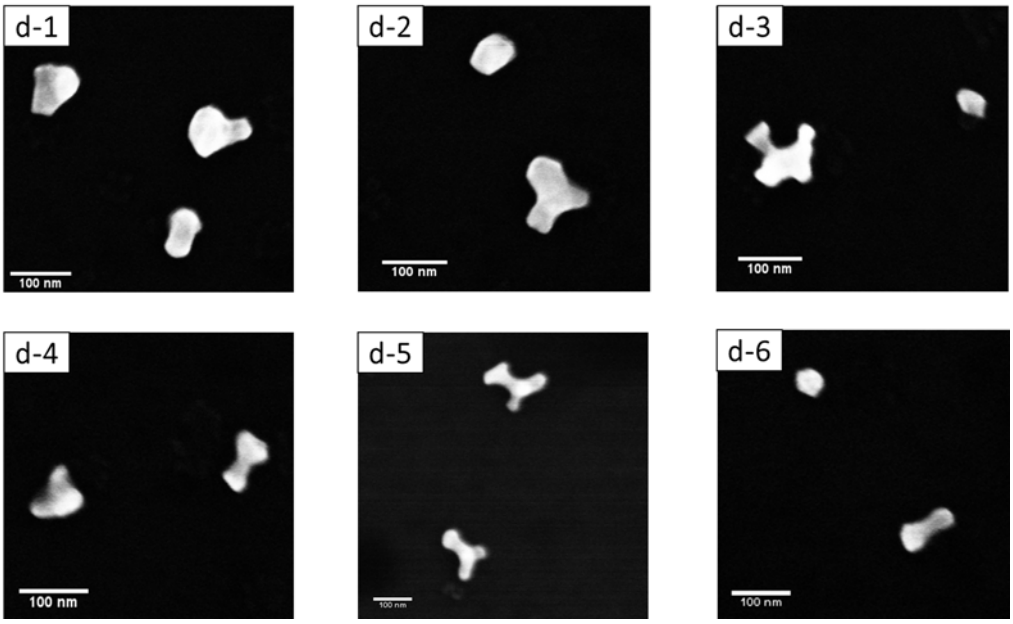

Figure S1. Additional SEM images of tripod Au nanoparticle suspensions with different reaction times of template dissolution (t_{dis}). T = 25 ˚C. (a) t_{dis} = 1 h. (b) t_{dis} =12 h. (c) t_{dis} = 24 h, without solvent replacement. (d) t_{dis} = 24 h, solvent replacement at t_{dis} = 12 h.

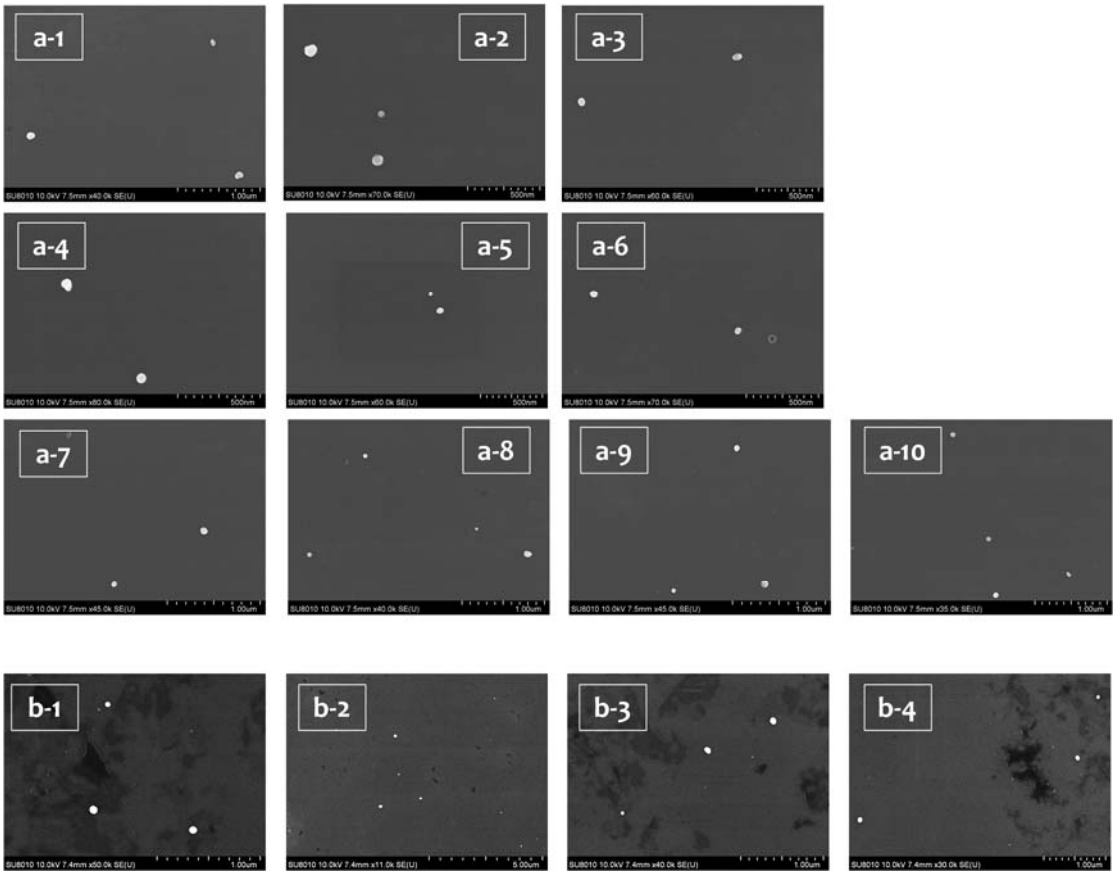

Figure S2. Additional SEM images of tripod Au nanoparticle suspensions with different annealing temperature (T). t_{dis} = 24 h. (a) T =300 ˚C. (b) T = 500 ˚C.

3. Emulsification measured by light scattering technique and visual inspection

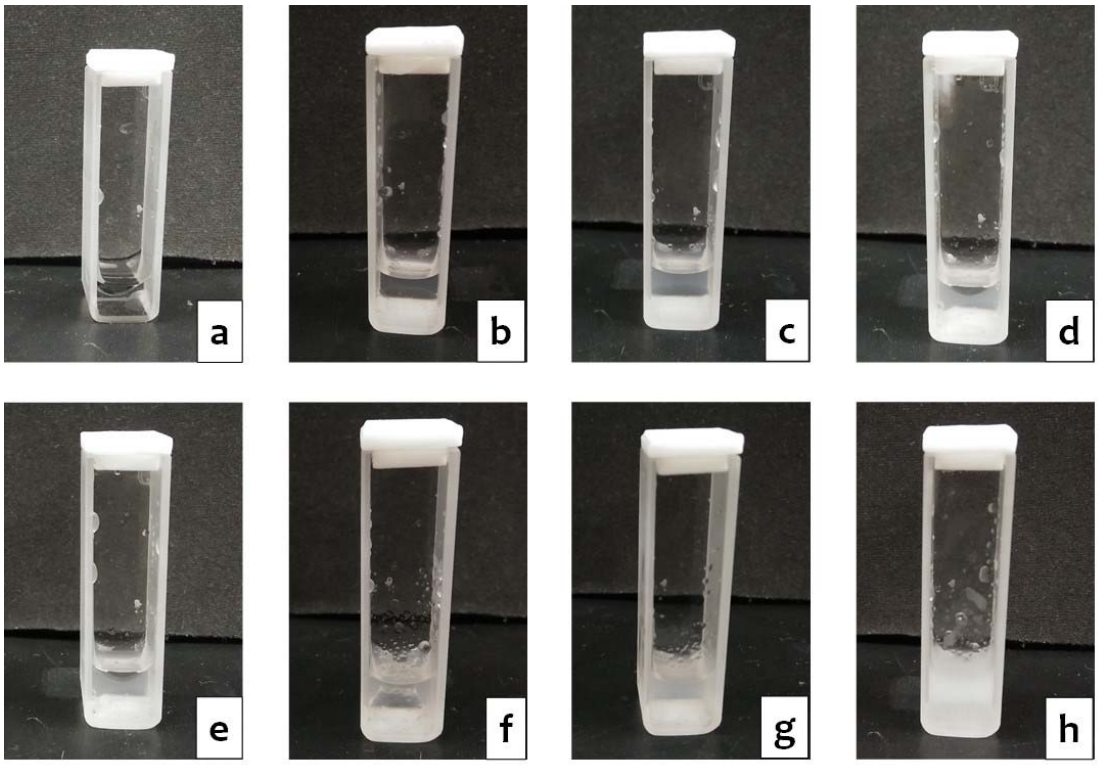

Figure S3. Visual inspection of the formation of DCM-in-water emulsion using PEG-SH as a stabilizer at different PEG-SH concentrations ($C_{PEG\text{-}SH}$). (a) $C_{PEG\text{-}SH}$ = 0μM. (b) $C_{PEG\text{-}SH}$ = 1 μM. (c) $C_{PEG\text{-}SH}$ = 2 μM. (d) $C_{PEG\text{-}SH}$ = 3 μM. (e) $C_{PEG\text{-}SH}$ = 4 μM. (f) $C_{PEG\text{-}SH}$ = 5 μM. (g) $C_{PEG\text{-}SH}$ = 10 μM. (h) $C_{PEG\text{-}SH}$ = 50 μM.

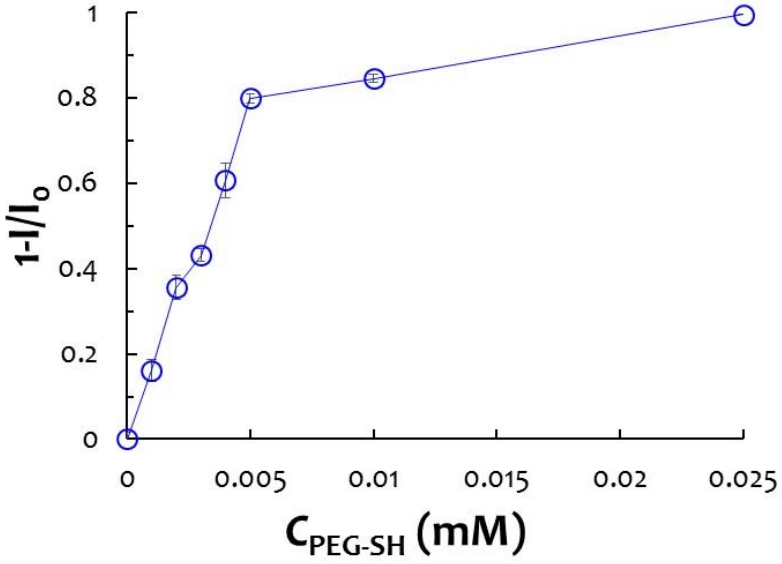

Figure S4. Analysis of the formation of DCM-in-water emulsion over various PEG-SH concentrations ($C_{PEG\text{-}SH}$) using light scattering techniques. The strong scattering intensity (low transmittance) indicates the formation of emulsion.

4. X-ray phototelectron spectroscopic (XPS) analysis

The X-ray photoelectron spectroscopy (XPS. PHI Quantera SXM, ULVAC-PHI, Chanhassen, MN, USA) was employed to obtain high-resolution spectra of S 2p for identifying the presence of PEG-SH corona on Au nano-tripod colloid. For comparison, commercial available 60 nm citrate-stabilized Au colloid (BBI Solutions, Cardiff, UK).was employed and conjugated with mercaptopropionic acid (MPA; to form a self-assembled monolayer).[4]

Figure S5 shows a XPS analysis (S 2p) of the PEG-SH-functionalized Au nano-tripods versus the MPA-conjugated Au nanoparticle. The signals of S 2p were clearly identified for the two samples, confirming the presence of sulfur on the Au nano-tripods. Note that the peak position at 168 eV for the S2p possesses higher value in comparing with that of the typical Au-S bond,[5,6] and the difference might be attributed to the relatively low signal-to-noise ratio and the discrepancies of instrument calibration. The unbound ligands were removed from both samples via centrifuge cleaning.

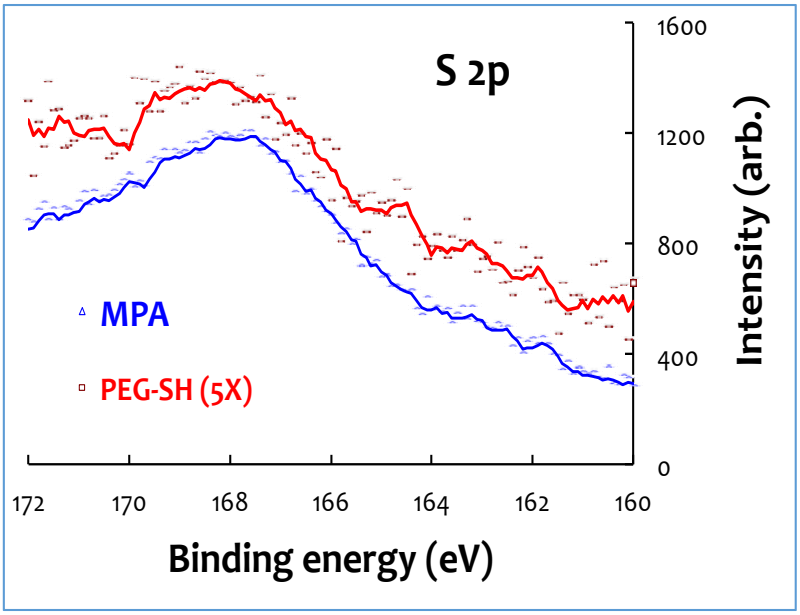

Figure S5. X-ray photoelectron spectroscopic (XPS) analysis of S 2p of PEG-SH-functionalized Au nano-tripods versus the mercaptopropionic acid (MPA)-conjugated colloidal Au nanoparticles.

5. Temperature-programmed electrospray-differential mobility analysis (TP-ES-DMA) for statistical analyses

The TP-ES-DMA measures the size distribution of tripod Au colloid based on the electrical mobility, providing a histogram-based representation of size.[6-9] Firstly, the tripod Au colloid was aerosolized and then charge-neutralized following a Boltzmann charge distribution.[6-9] For equal concentrations of positive and negative ions, the fraction of particles f_n of a given $d_{p,m}$ having n positive elementary units of charge can be calculated using Eq. S1:[7,10]

$$f_n = \frac{\exp(\frac{K_E n^2 e^2}{d_{p,m} kT})}{\sum_{n=-\infty}^{\infty} \exp(\frac{K_E n^2 e^2}{d_{p,m} kT})} \quad \text{(S1)}$$

Here K_E is a constant of proportionality (=9.0*10^9 N*m^2*C^{-2}). For example, $f_n \approx 10$ % for 30 nm-sized particles. When $d_{p,m} < 100$ nm, the singly positively-charged particles were the main species to be classified and counted through the scanning of the electric field of DMA.[9] After charge correction, Figure 2b of the main text can be converted to Figure S6 (i.e., without the normalization of number density).

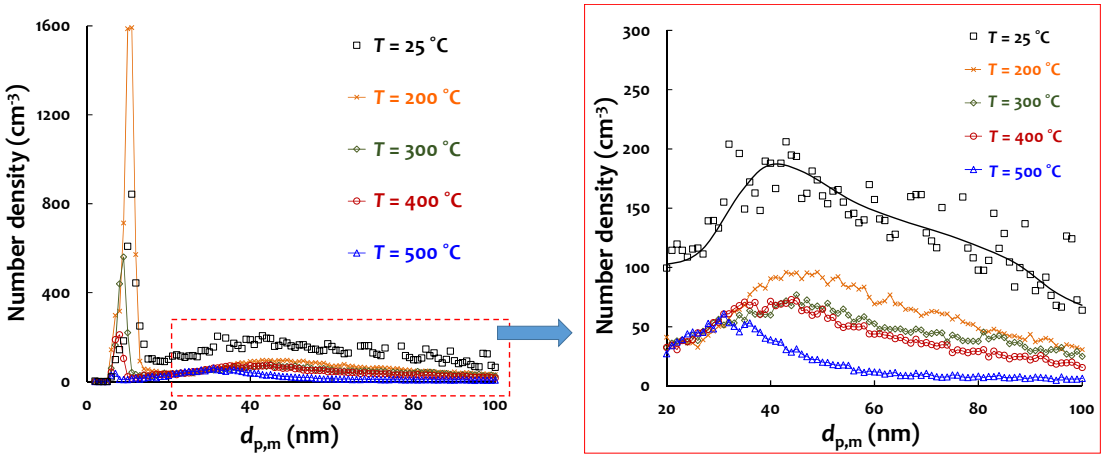

Figure S6. Mobility size distributions of tripod AuNP colloid measured by TP-ES-DMA, after charge correction.

In principal, the particles counted with a selected mobility size ($d_{p,m}$) have a mobility diameter ranging from ($d_{p,m}$ - $\Delta d_{p,m}$) to ($d_{p,m}$ + $\Delta d_{p,m}$) following a transfer function of DMA. Here the $\Delta d_{p,m}$ is simplified as ($Q_{aerosol}/Q_{sheath}$) × $d_{p,m}$, which is determined by the chosen aerosol flow rate ($Q_{aerosol}$) to the sheath flow rate of DMA (Q_{sheath}). In this study, $\Delta d_{p,m} = 0.1\ d_{p,m}$.

The number of particle counts in each group (n_{dp}) can be obtained using Eq. S2:

$$n_{dp} = N_{p,g,dp} * Q_{aerosol} * t_{scan} \quad \text{(S2)}.$$

Here $N_{p,g,dp}$ is the number density of particles at a specific $d_{p,m}$, which can be obtained from Figure S6 (unit: cm^{-3}). t_{scan} is the time for particle counting at each size step (10 s in this study). After the summation of the groups ranging from $d_{p,m} = 15$ nm to $d_{p,m} = 100$ nm, the total number of particle counts were calculated as 2.3×10^6 for T= 25 °C, 9.5×10^5 for $T = 200$ °C, 7.4×10^5 for $T = 300$ °C, 6.5×10^5 for $T = 400$ °C, 3.2×10^5 for $T = 500$ °C.

6. Derivation of stability ratio of tripod AuNP

The aggregation rate constant (k_D) can be determined based on the change of mobility size distributions versus storage time. Figure S7 shows the mobility size distribution of unconjugated Au nanoparticles in an ammonium acetate aqueous

solution (≈4 mmol/L).[6] The formation of dimer, trimer and tetramer was observed, and the k_D was calculated as ≈ 10^{-17} cm^3/s. Since the particle size distribution of tripod AuNP suspension was relatively unchanged after 7 days, the k_D of tripod AuNP in the 4 mmol/L acetate aqueous solution can be estimated to be < 10^{-17} cm^3/s.

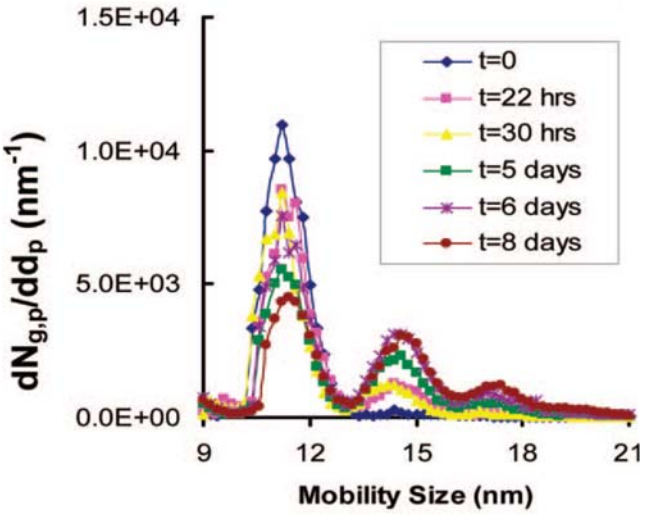

Figure S6. Mobility size distribution of unconjugated Au nanoparticle in an ammonium acetate aqueous solution (≈4 mmol/L).[6]

The dimensionless stability ratio can be determined using Eq, S3,[6]

$$W \equiv k_D^{fast}/k_D \qquad \text{(S3)}.$$

Here k_D^{fast} is the flocculation rate constant driven solely by Brownian motion. [6] In principal, a larger value of W corresponds to a more stable suspension. By calculation, $W > 10^6$ for tripod AuNP suspension in our study.

7. Derivation of the mobility diameter, average dynamic shape factor and the extent of polydispesity

The particle size is determined by measuring the terminal velocity of the particle (V_t) in a direct circuit field (E),

$$V_t = \frac{neC_c}{3\pi\mu d_{p,m}} E \qquad \text{(S4)}.$$

Where $d_{p,m}$ is the mobility diameter of a particle by assuming particle is spherical with equivalent electrical mobility to sphere. μ is the viscosity of air, and C_c is the Cunningham slip correction, which is calculated using Eq. S5:[7,10]

$$C_c = 1 + K_n[\alpha + \beta \exp(-\gamma/K_n)] \qquad \text{(S5)}.$$

Here $\alpha = 1.142$, $\beta = 0.558$, $\gamma = 0.999$. $K_n = 2\lambda/d_{p,m}$, where λ is the gas mean free path (≈66 nm for air at room temperature). The electrical mobility (Z_e) of the measured aerosol particles is expressed as Eq. S6:[7]

$$Z_e = \frac{V_t}{E} = \frac{neC_c}{3\pi\mu d_{p,m}} \qquad \text{(S6)}$$

Based on the design of electrostatic classifier, polarity of electric field (negative), and carrier gas flow rate, the measured Z_e is expressed as Eq. S7,[9]

$$Z_e = Q_{sh}/(2\pi V_{DMA} L)*\ln(r_2/r_1) \qquad \text{(S7)},$$

where Q_{sh} is the flow rate of sheath air in DMA, L is the length between exit slit and polydisperse aerosol inlet, and V_{DMA} is the applied DC voltage to the DMA. r_2 and r_1 are outer and inner radius of DMA, respectively.[9] Combining Eq. S6 and S7, we obtain a correlation of $d_{p,m}$ as a function of V_{DMA}.

The dynamic shape factor (χ) is defined as the ratio of the actual resistance force of the non-spherical particle ($F_D = \frac{3\pi\mu d_{p,m} v_t}{C_c}$) to the resistance of a sphere having the same volume as that of the non-spherical particle (i.e., $F_D = \frac{3\pi\mu d_e v_t}{C_c}$). $d_{e,n}$ is the number-average equivalent-volume diameter (d_e) of the Au nano-tripod, which has the same volume as that of the non-spherical particle.[7] As a results, $\chi = d_{p,m}/d_{e,n}$.

The extent of polydispesity (*P.I.*) is developed as an indicator to the uniformity of templated Au nanomaterial on a basis of volume (i.e., the amount of deposited Au per particle), which is defined as the ratio of the width of volume-based distribution to the volume-average diameter. As shown in the Figure 2b, the Au nano-tripod sintered to sphere after a gas-phase thermal treatment at 500 ˚C. Hence a d_e-based size distribution

was obtained at T = 500 ˚C, which can be used to calculate the *P.I.* by Eq. 2 of the main text.

Reference

(1) R. M. Ho, C. K. Chen, Y. W. Chiang, B. T. Ko, C. C. Lin, *Adv Mater* 2006, *18*, 2355.
(2) H. Y. Hsueh, H. Y. Chen, Y. C. Hung, Y. C. Ling, S. Gwo, R. M. Ho, *Adv Mater* 2013, *25*, 1780.
(3) H. F. Wang, H. W. Wang, R. M. Ho, *Chem Commun* 2012, *48*, 3665.
(4) D. H. Tsai, F. W. DelRio, R. I. MacCuspie, T. J. Cho, M. R. Zachariah, V. A. Hackley, *Langmuir* 2010, *26*, 10325.
(5) D. H. Tsai, T. J. Cho, F. W. DelRio, J. M. Gorham, J. W. Zheng, J. J. Tan, M. R. Zachariah, V. A. Hackley, *Langmuir* 2014, *30*, 3397.
(6) D. H. Tsai, R. A. Zangmeister, L. F. Pease, M. J. Tarlov, M. R. Zachariah, *Langmuir* 2008, *24*, 8483.
(7) W. C. Hinds *Aerosol Technology: Properties, Behavior, and Measurement of Airborne Particles*; Second ed.; John Wiley & Sons, 1999.
(8) D. H. Tsai, L. F. Pease, R. A. Zangmeister, M. J. Tarlov, M. R. Zachariah, *Langmuir* 2009, *25*, 140.
(9) J. T. Tai, Y. C. Lai, J. H. Yang, H. C. Ho, H. F. Wang, R. M. Ho, D. H. Tsai, *Analytical Chemistry* 2015, *87*, 3884.
(10) J. M. Berg, A. Romoser, N. Banerjee, R. Zebda, C. M. Sayes, *Nanotoxicology* 2009, *3*, 276.